# COMPACT HIGH–VELOCITY CLOUDS AT HIGH RESOLUTION

W.B. BURTON
*Sterrewacht Leiden*
*P.O. Box 9513, 2300 RA Leiden, The Netherlands*

AND

R. BRAUN
*Netherlands Foundation for Research in Astronomy*
*P.O. Box 2, 7990 AA Dwingeloo, The Netherlands*

**Abstract.** Six examples of the compact, isolated high–velocity clouds catalogued by Braun & Burton (1999) and identified with a dynamically cold ensemble of primitive objects falling towards the barycenter of the Local Group have been imaged with the Westerbork Synthesis Radio Telescope; an additional ten have been imaged with the Arecibo telescope. The imaging reveals a characteristic core/halo morphology: one or several cores of cool, relatively high–column–density material, are embedded in an extended halo of warmer, lower–density material. Several of the cores show kinematic gradients consistent with rotation; these CHVCs are evidently rotationally supported and dark–matter dominated. The imaging data allows several independent estimates of the distances to these objects, which lie in the range 0.3 to 1.0 Mpc. The CHVC properties resemble what might be expected from very dark dwarf irregular galaxies.

## 1. Introduction

Hierarchical structure formation scenarios suggest that galaxies form by continuous accretion of small, dark–matter dominated satellites. The possibility of an extragalactic deployment of high–velocity clouds has long been considered, and in various contexts, by Oort (1966, 1970, 1981), Verschuur (1975), Eichler (1976), Einasto et al. (1976), Bajaja et al. (1987), Burton (1997), Wakker & van Woerden (1997), Braun & Burton (1999; 2000, astro-ph/9912417), Blitz et al. (1999), and López–Corredoira et al. (1999). The discussion of Blitz et al. ties several HVC properties to the hierarchical structure formation and evolution of galaxies. In this context the extended
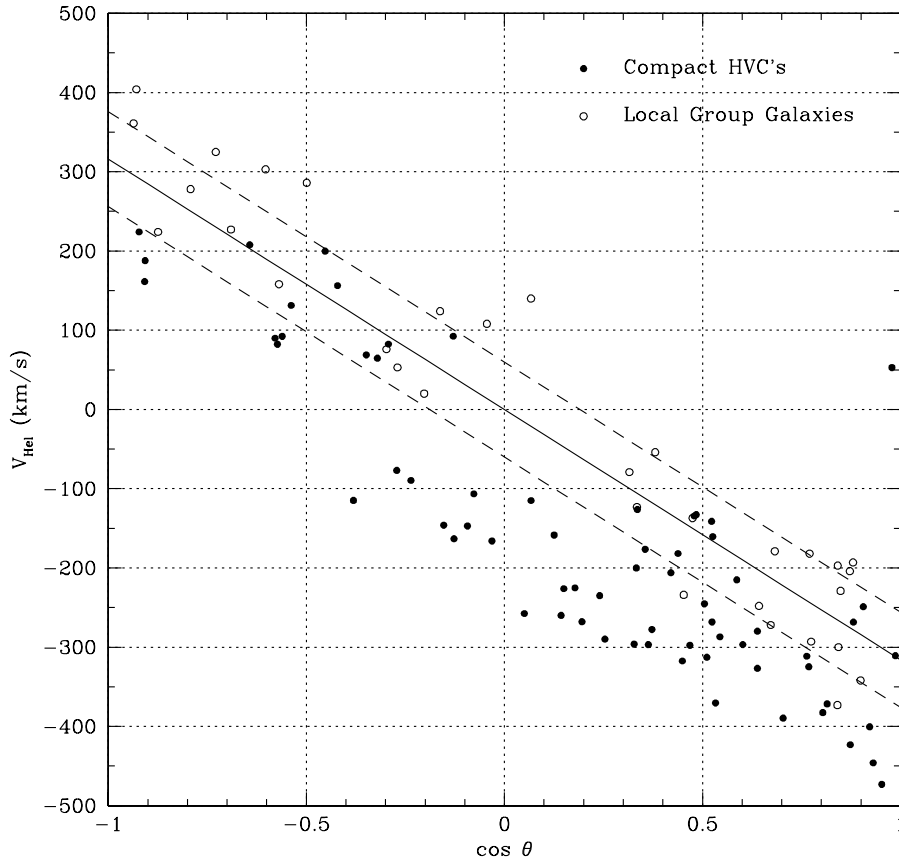
*Figure 1.* Variation of heliocentric velocity versus the cosine of the angular distance between the solar apex and the $(l, b)$ direction of the compact, isolated high-velocity clouds catalogued by Braun & Burton (1999). The CHVCs are represented by filled circles; the galaxies constituting the Local Group, by open circles. The solid line represents the solar motion of $v_\odot = 316$ km s$^{-1}$ toward $l = 90°$, $b = -4°$ (Karachentsev & Makarov 1996). The dashed lines represent the envelope one standard deviation ($\pm 60$ km s$^{-1}$; Sandage 1986) about the velocity/angular–distance relation, pertaining for galaxies believed to be members of the Local Group. The kinematic and spatial deployment of the CHVCs is consistent with that of a dynamically cold ensemble spread throughout the Local Group, with a net infall velocity towards the barycenter of the Local Group of some 100 km s$^{-1}$.

HVC complexes would be nearby and currently being accreted onto the Galaxy, while the compact, isolated objects would be the primitive building blocks at larger distances, scattered throughout the Local Group.

The class of compact, isolated high–velocity clouds catalogued by Braun & Burton (1999) represent objects which plausibly originated under common circumstances, have shared a common evolutionary history, have not

(yet) been strongly influenced by the radiative or tidal fields of the Milky Way or M31, and are falling towards the Local Group barycenter. The CHVC catalogue was based on survey data made with telescopes of modest resolution. The principal source was the Leiden/Dwingeloo Survey (LDS) of Hartman & Burton (1997), characterized by the angular resolution of $36'$ provided by the Dwingeloo 25–meter antenna; important additional data came from the more coarsely–sampled surveys of Hulsbosch & Wakker (1988) and of Bajaja et al. (1985) as analyzed by Wakker & van Woerden (1991), as well as from some new H I material observed at $21'$ resolution using the NRAO 140–foot telescope. The CHVCs are largely unresolved in angle in the single–dish catalogue, and therefore the large range in observed velocity widths can not be directly interpreted in terms of the intrinsic properties of individual gaseous entities.

Of the sample of 65 CHVCs catalogued by Braun & Burton (1999) only two had been subject earlier to interferometric imaging. Wakker & Schwarz had used the WSRT to show that both CHVC $114-10-430$ and CHVC $114-06-466$ exhibit a core/halo structure (with only some 40% of the single–dish flux recovered) that the linewidths of the resolved cores were substantially narrower than when the individual cores were blended at low resolution, and that several of the components displayed systematic velocity gradients. We have now imaged six additional CHVC fields using the Westerbork Synthesis Radio Telescope, and a further ten using the 304–meter Arecibo telescope. Selected properties of several of these fields are shown here. A complete discussion of the WSRT imaging is given by Braun & Burton (2000, astro-ph/9912417); a discussion of the Arecibo material is in preparation.

## 2. WSRT and Arecibo Data

Observations of the six CHVC fields imaged with the WSRT involved twelve–hour integrations in the standard array configuration having a shortest baseline of 36 meters. The effective velocity resolution was 1.2 times the channel spacing of 2.06 $\mathrm{km\,s^{-1}}$, over 256 spectral channels centered on the $v_{\mathrm{LSR}}$ of each source as catalogued by Braun & Burton (1999) on the basis of the single–dish spectra in the LDS. The angular and kinematic resolution afforded by the WSRT makes it well suited in important regards to detailed studies of the CHVC class of objects. Diffuse structures extending over more than about 10 arcmin are, however, not adequately imaged by the interferometer unless precautions are taken to eliminate the short–spacing bowl surrounding regions of bright extended emission. In a straightforward attempt to identify the column densities and overal extent likely to characterize any diffuse structures, we made use of the LDS data to determine
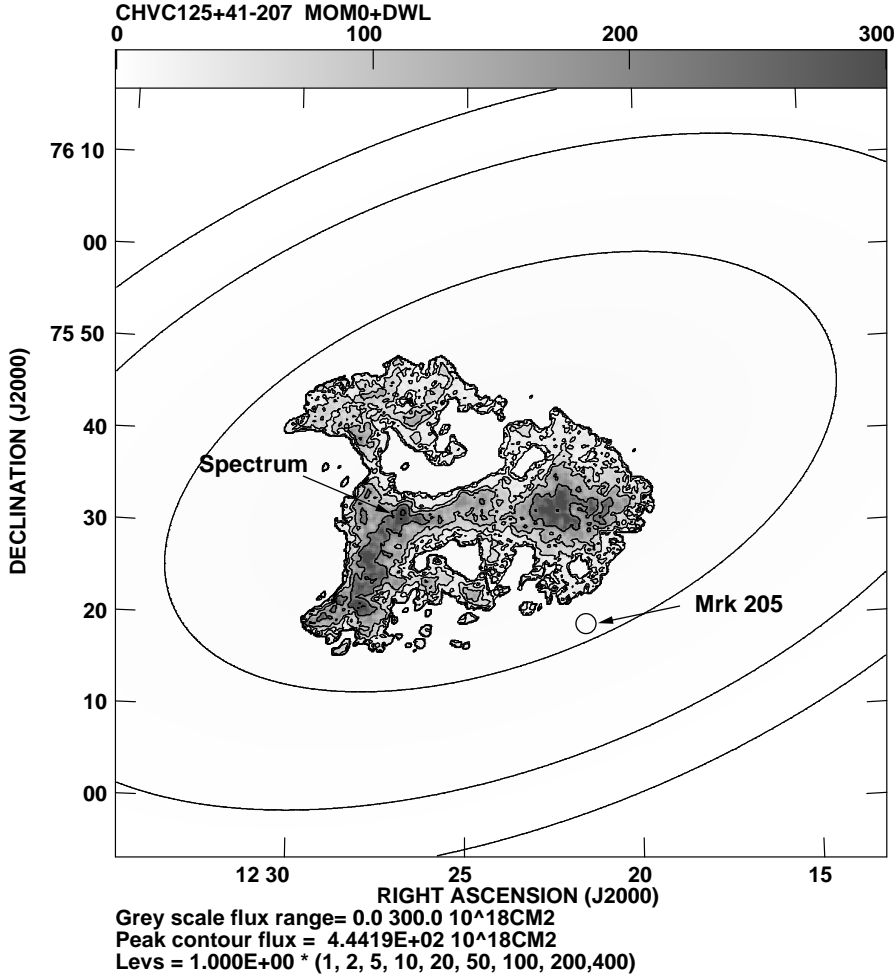
CHVC125+41-207  MOM0+DWL

Figure 2. WSRT image of CHVC 125+41–207 displaying H I column densities at 28 arcsec angular resolution. $N_{HI}$ was calculated assuming negligible opacity, and is displayed by contours at the levels indicated in units of $10^{18}$ cm$^{-2}$ and a linear grey–scale running from 0 to $300 \times 10^{18}$ cm$^{-2}$. The location of the Seyfert galaxy Mrk 205 is marked. This background source lies on a line of sight which penetrates the halo of the CHVC, where reconstruction of the integral flux using the composite WSRT and LDS single–dish data reveals a moderate diffuse–emission column depth. Bowen & Blades (1993) have measured Mg II absorption towards Mrk 205, and a metallicity substantially subsolar.

the emission from an elliptical Gaussian with dimensions and orientation as measured in the LDS, and with a total flux sufficient to recover the LDS integrated emission.

We have also recently observed ten CHVCs with the Arecibo telescope. The Arecibo facility is well–suited to provide sensitivity to the total column
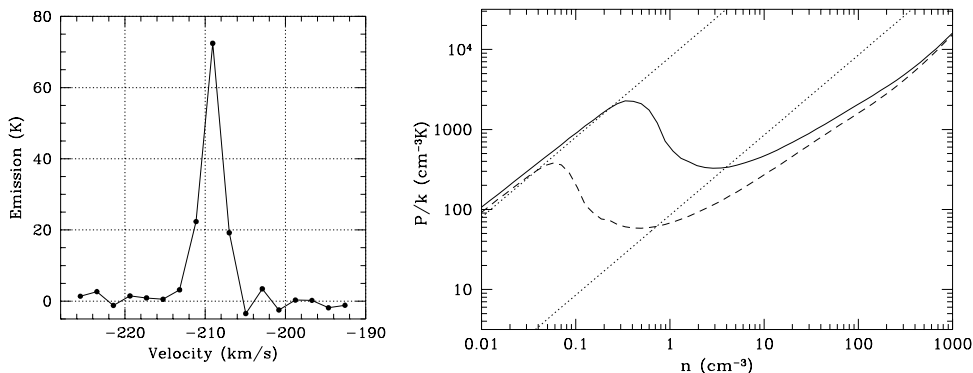
*Figure 3.*    *left:* H I spectrum observed in the direction indicated in Fig. 2 of one of the bright emission knots in CHVC 125+41−207 . The spectrum is unresolved at a channel separation of 2 km s$^{-1}$, indicating a core temperature of less than 85 K and quiescent turbulence. *right:* Equilibrium temperature curves for H I in an intergalactic environment characterized by a metallicity of 10% of the solar value and a dust–to–gas ratio of 10% of that in the solar neighborhood, calculated for two values of the neutral shielding column depth, namely $10^{19}$ cm$^{-2}$ (solid line) and $10^{20}$ cm$^{-2}$ (dashed line). The upper dotted line indicates the 8000 K temperature characteristic of the WNM; the lower one, the kinetic temperature of 85 K observed in the opaque core of CHVC 125+41−207. The volume density is tightly constrained for this temperature; a distance then follows from the measured column density and angular size.

density at relatively high resolution. This is especially important for CHVC targets which are of a size comparable to the field of view of most synthesis intruments. The Arecibo targets were observed with the new Gregorian feed and the narrow L–band receiver with two bandpass settings, namely 6.25 MHz and 1.56 MHz (yielding $\Delta v = 1.3$ and 0.32 km s$^{-1}$, respectively) each centered on the $v_{\mathrm{LSR}}$ of the CHVC as determined by Braun & Burton (1999). The Arecibo targets were first mapped on a grid of $1° \times 1°$ size on a fully–sampled 90 arcsec lattice, in short integrations, in order to determine the locations of the peak flux concentrations; then at one or more of these principal components long–integration spectra were accumulated in a cut made at constant declination by repeating drift scans over the same $2°$ in right ascension. Typical column density sensitivies of some $10^{17.5}$ cm$^{-2}$ over 20 km s$^{-1}$ were reached, an $N_{\mathrm{HI}}$ regime largely unexplored (cf. Zwaan et al. 1997).

## 3.   The Exceptionally Narrow Core in CHVC 125+41−207

The compact high–velocity cloud CHVC 125+41−207 is typical of the class of objects in several regards. Figure 2, adopted from Braun & Burton (2000, astro-ph/9912417; see also Burton & Braun 1999) shows several cool, quiescent cores embedded in a diffuse, warmer halo. The spectrum plotted in

Fig. 3, observed towards the brightest of these cores, has a linewidth which is completely unresolved by the effective resolution of the WSRT imaging. The velocity channels adjacent to the line peak have intensities below 20% of the maximum value. Such a width is one of the narrowest measured in H I emission, and contrains both the kinetic temperature and the amount of turbulence. An upper limit to the thermal–broadening FWHM of 2 $\mathrm{km\,s^{-1}}$ corresponds to an upper limit to the kinetic temperature of 85 K. The physical situation is yet more tightly constrained, because the brightness temperature in this core is observed to be 75 K; thus a lower limit to the opacity follows from $T_\mathrm{b} = T_\mathrm{k}(1 - e^{-1})$, yielding $\tau \geq 2$. Any broadening which might be due to macroscopic turbulence is less than 1 $\mathrm{km\,s^{-1}}$.

The tightly–constrained temperature found for CHVC $125+41-207$ allows an estimate of the distance to this object. Wolfire et al. (1995a, 1995b) show that a cool H I phase is stable under extragalactic conditions if a sufficient column of shielding gas is present and if the thermal pressure is high. Calculations of equilibrium conditions which would pertain in the Local Group environment have been communicated to us by Wolfire, Sternberg, Hollenbach, and McKee, and are shown in Fig. 3 for two bracketing values of the shielding column density, namely $10^{19}$ cm$^{-2}$ and $10^{20}$ cm$^{-2}$. The figure shows that the equilibrium volume densities corresponding to the observed value of $T_\mathrm{k} = 85$ K lie in the range 0.65 to 3.5 cm$^{-3}$. Thus provided with this range of volume densities, and having measured both the column depth of the cool core and its angular size, the distance to CHVC $125+41-207$ follows directly from $D = N_\mathrm{HI}/(n_\mathrm{HI}/\theta)$, yielding a value in the range 210 to 1100 kpc. Further considerations of several opaque, cool cores made by Braun & Burton (2000, astro-ph/9912417) suggest that a distances between 0.5 and 1 Mpc are most plausibly representative of these objects.

Measurements of metallicity of high–velocity clouds are important to discussions of the nature of the phenomenon. If the clouds are primitive objects scattered throughout the Local Group, the gas would not be substantially enriched in heavy elements produced by stellar evolution. On the other hand, if the anomalous velocities had been generated by supernova explosions or some other energetic occurance in the Galactic disk, for example according to the precepts of the galactic fountain scenario (Shapiro & Field, 1976; Bregman, 1980) then the gas would be substantially enriched, with the already moderately high metallicities characteristic of the Galactic disk further enhanced by the circumstances of the ejection event. The small angular size of the CHVCs, and the amount of substructure being revealed at high resolution, will make it generally difficult to find suitable background sources. But the diffuse halo of CHVC $125+41-207$ overlaps the Seyfert galaxy Mrk 205, and in this direction Bowen & Blades (1993) de-
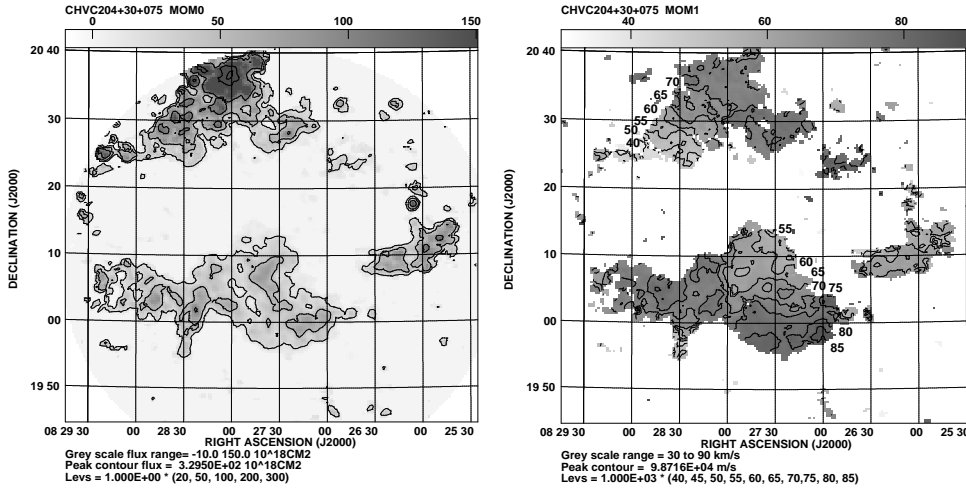
*Figure 4.* *left:* Westerbork image of CHVC 204+30+075 showing $N_{\rm HI}$ (calculated assuming negligible opacity) at an angular resolution of 1 arcmin; contours are drawn at levels of 20, 50, 100, 200, and $300 \times 10^{18}$ cm$^{-2}$. *right:* Intensity–weighted line–of–sight velocity, with contours of $v_{\rm LSR}$ showing systematic kinematic gradients across the two principal components of the CHVC object, consistent with rotation; contours are drawn in steps of 5 km s$^{-1}$ from 40 to 85 km s$^{-1}$.

tected Mg II absorption at $v_{\rm LSR} = -209$ km s$^{-1}$. We determine a metallicity of this object in the range 0.04 to 0.07 solar.

## 4. Rotation in the Cores of CHVC 204+30+075

The narrowest FWHM of the CHVCs cataloged by Braun & Burton had a value of 5.9 km s$^{-1}$; the broadest, a value of 95 km s$^{-1}$. Under higher resolution, the characteristic width narrows as objects are resolved into several principal components, moving relative to each other. If the objects with multiple cores are to be stable, distances of order several hundred kpc are required. Some of the compact cores imaged owe their large total width in the LDS single–dish data to velocity gradients. The resolved WSRT image of CHVC 204+30+075 is shown in Fig. 4. The object shows two principal components each of which is elongated; furthermore, each of the elongated structures shows a systematic velocity gradient along the major axis.

The velocity gradients exhibited by the two principal components of CHVC 204+30+075 can be modelled in terms of circular rotation in a flattened disk system. Fig. 5 shows the results of fitting a standard tilted–ring model to the data. The fits display velocity rising slowly but continuously
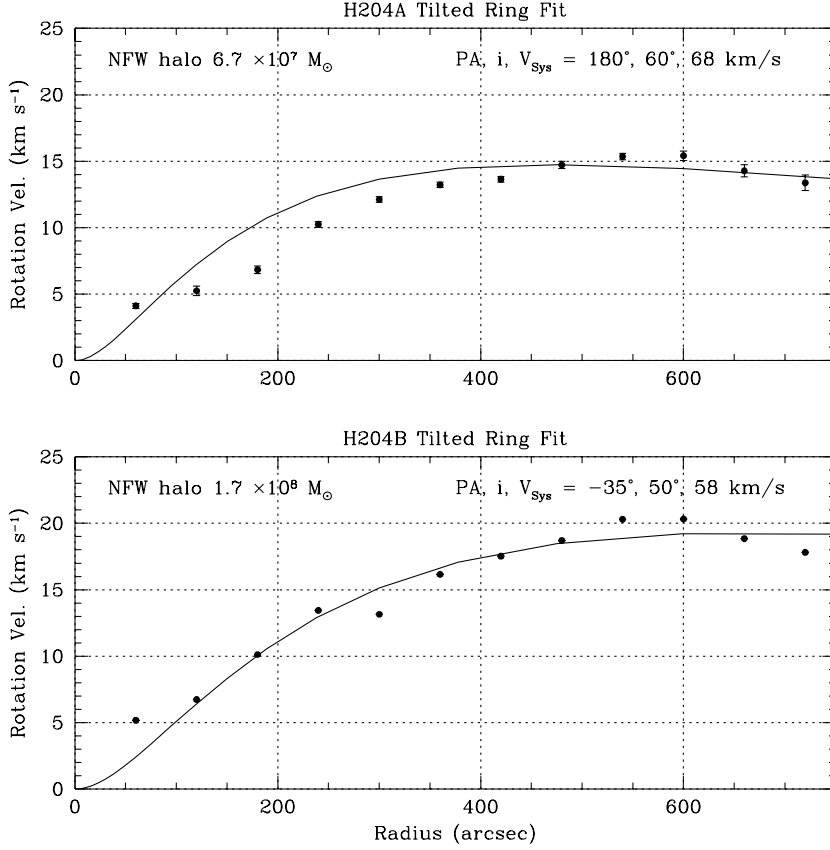
*Figure 5.* Rotation velocities fit by a standard application of the tilted–ring method to kinematic gradients revealed in the two principal components of CHVC 204+30+075 shown in Fig. 4. (The upper panel pertains to the component at higher declination.) The best–fit position angle, inclination, and systemic velocity are indicated. The solid lines show the rotation curves of Navarro, Frenk, & White (1997) cold–dark–matter halos of the indicated masses.

with radius to an amplitude of some $15 \, \mathrm{km \, s^{-1}}$ in the one case and to some $20 \, \mathrm{km \, s^{-1}}$ in the other, and then flattening to a constant value beyond about 500 or 600 arcsec. Estimates of the contained dynamical mass follow from the rotation curves if the distance is assumed, and the total gas mass follows from the integrated H I fluxes. At an assumed distance of 0.7 Mpc, the two principal clumps of CHVC 204+30+075 have $M_{\mathrm{dyn}} = 10^{8.1}$ and $10^{8.3}$ $\mathrm{M_\odot}$, and gas masses (including H I and helium of 40% by mass) of $10^{6.5}$ and $10^{6.9} \, \mathrm{M_\odot}$, respectively for the upper and lower concentrations shown in Figures 4 and 5. The dark–to–visible mass ratios for these concentrations are 36 and 29, respectively.
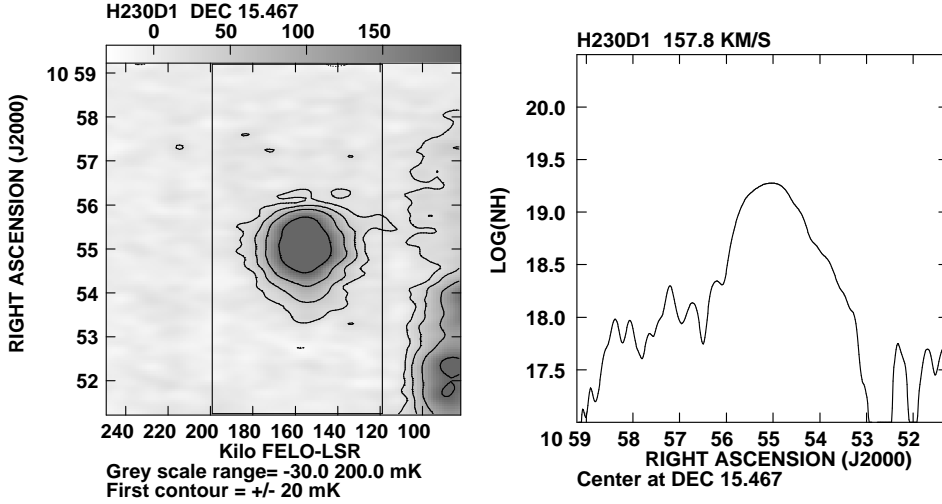
*Figure 6.* *left:* Position, velocity cut through CHVC 230+61+165 observed with the Arecibo telescope, at an angular resolution of 3′.3. The cut samples right ascension along the fixed declination 15°.467. This compact object shows no kinematic gradient along the cut sampled. *right:* Variation of $N_{HI}$ with position, sampled at the velocity (158 km s$^{-1}$) of the peak of the column–density distribution. The $N_{HI}$ values plotted here and in Fig. 7 are based on calibrated intensities in units of $T_b$.

The shape of the modelled rotation curves for both of the CHVC 204+30+075 components is reproduced by the standard cold–dark–matter halo as presented by Navarro et al. (1997). At the assumed distance of 0.7 Mpc, the Navarro et al. halos fit to the two components have masses of $10^{7.8}$ M$_\odot$ (within 9.3 kpc) and $10^{8.2}$ M$_\odot$ (within 12.6 kpc), respectively.

## 5.  The Objects CHVC 230+61+165 and CHVC 158−39−285

The WSRT imaging of CHVC 230+61+165 revealed a simple, faint structure. The Arecibo telescope is particularly well-suited to such targets, because of its sensitivity to low H I brightnesses. A position, velocity cut through this object at the location of the peak $N_{HI}$ is shown in the lefthand panel of Fig. 6. No kinematic gradient is revealed. However the cut does show an interesting characteristic which several other of the CHVCs observed at Arecibo also show, namely a tendency to be more sharply bounded on one side of the cut than on the other. In the case of CHVC 230+61+165, the higher right–ascension boundary is sharper than the lower one down to $N_{HI} = 10^{18.5}$. (We will consider this property further in our full discussion of the Arecibo observations.)

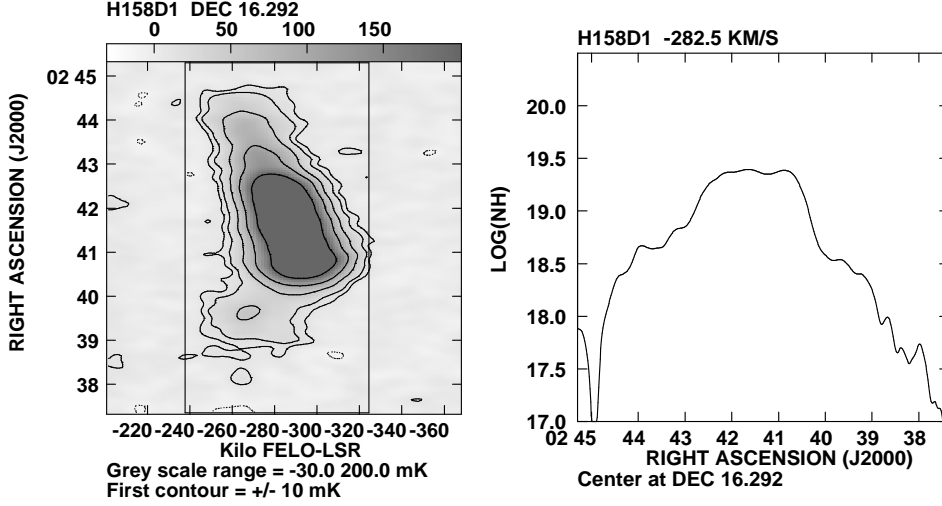The Arecibo data on CHVC 158−39−285 are shown in Fig. 7. This

*Figure 7.* *left:* Position, velocity cut through CHVC $158-39-285$ observed with the Arecibo telescope at an angular resolution of $3'.3$. The cut samples right ascension along the fixed declination $16°.292$. This CHVC shows a kinematic gradient consistent with rotation, spanning some $40 \text{ km s}^{-1}$, as well as the characteristic core/halo morphology. *right:* Variation of $N_{HI}$ with position, sampled at the velocity $(-282.5 \text{ km s}^{-1})$ of the peak of the column–density distribution.

object is also a simple one, with only one component revealed. The position, velocity cut through the location of the peak $N_{HI}$ value also shows that one side of the object is more sharply bounded than the other. The prominent kinematic gradient is consistent with simple rotation within the high $N_{HI}$ core. The plots on the righthand panels of Fig. 6 and Fig. 7 show the variation of $N_{HI}$ with position across the two CHVCs. The cores are embedded in diffuse material with characteristic $N_{HI}$ values of order $10^{18.5}$ cm$^{-2}$.

## 6. Discussion

The WSRT and Arecibo high–resolution imaging shows that the morphology of the compact high–velocity clouds is characterized by one or more quiescent, low–dispersion compact cores embedded in a diffuse, warmer halo. The gas in the cores is identified with the cool neutral medium (CNM) of condensed H I at temperatures in the range $50 - 200$ K; the halo gas is identified with the warm neutral medium. Such a nested geometry is expected if the CNM is to be stable in the presence of an ionizing radiation field of the sort expected in the Local Group environment. The cores contribute typically about 40% of the H I flux, while covering about 15% of the surface

in the CHVC.

The high–resolution imaging data allows two independent distance estimates to be made. A distance for CHVC 125+41−207 follows from assuming rough spherical symmetry and equating the well–constrained volume and column densities of the compact cores. Another distance constraint (coupled with a dark–to–visible mass ratio) follows from consideration of the stability of CHVCs having multiple cores in a common envelope but having large relative velocities. The evidence available indicates that CHVCs have characteristic sizes of about 10 kpc, H I masses of about $10^7$ M$_\odot$, and are at distances of 0.4 − 1.0 Mpc.

The imaging has also shown that the compact cores of CHVCs are commonly rotating. The observed kinematic gradients can be fit by rotating flattened disks, yielding dynamical masses for assumed distances. Dark–to–visible mass ratios of order 10 − 40 at $D = 0.7$ Mpc are indicated. The rotation curves shown here agree well with the cold–dark–matter halo predicted by Navarro et al. (1997).

The gaseous properties characteristic of CHVCs bear similarities to those of many dwarf irregular galaxies populating the Local Group (e.g. Young & Lo 1996, 1997a, 1997b). It is an important astrophysical challenge to establish the details of these similarities. It is particularly important to establish whether any of the CHVCs contain stars as well; the stellar density might be very low, but detection of any stellar component would lead to improved distances and would constrain the evolutionary history, and would augment the information on the faint end of the Local Group luminosity function. Failure to detect stars would imply that CHVCs are very primitive proto–galactic objects dominated by dark–matter halos. In either case, it seems plausible that the CHVCs are the missing Local Group satellite systems predicted by Klypin et al. (1999) and Moore et al. (1999).

### Acknowledgements

# References

1.  Bajaja, E., Cappa de Nicolau, C.E., Cersosimo, J.C., Loiseau, N., Martin, M.C., et al., 1985, *ApJS*, **58**, 143
2.  Bajaja, E., Morras, R., and Pöppel, W.G.L., 1987, *Pub. Astr. Inst. Czech. Ac. Sci.*, **69**, 237
3.  Blitz, L., Spergel, D.N., Teuben, P.J., Hartmann, D., and Burton, W.B., 1999, *ApJ*, **514**, 818
4.  Bowen, D.V., and Blades, J.C., 1993, *ApJ*, **403**, L55
5.  Braun, R., and Burton, W.B., 1999, *A&A*, **341**, 437
6.  Braun, R., and Burton, W.B., 2000, *A&A* (submitted); astro-ph/9912417
7.  Bregman, J.N., 1980, *ApJ*, **236**, 577
8.  Burton, W.B., 1997, in *The Physics of the Galactic Halo*, eds. Lesch H., Dettmann R.-J., Mebold U., Schlickeiser R. (Berlin: Akademie Verlag), 15
9.  Burton, W.B., and Braun, R. 1999, *Nature*, **402**, 359
10. Eichler, D., 1976, *ApJ*, **208**, 694
11. Einasto, J., Haud, U., Jôeveer, M., and Kaasik, A., 1976, *MNRAS*, **177**, 357
12. Giovanelli, R., 1981, *AJ*, **86**, 1468
13. Hartmann, D., and Burton, W.B., 1997, *Atlas of Galactic Neutral Hydrogen*. Cambridge University Press, Cambridge
14. Karachentsev, I.D., and Makarov, D.A., 1996, *AJ*, **111**, 794
15. Klypin, A., Kravtsov, A.V., Valenzuela, O., and Prada, F., 1999, *ApJ*, **522**, 82
16. López–Corredoira, M., Beckman, J.E., and Casuso, E., 1999, *A&A*, **351**, 920
17. Moore, B., Ghigna, S., Governato, G., Lake, G., Quinn, T., Stadel, J., and Tozzi, P., 1999, *ApJ*, **524**, 19
18. Navarro, J.F., Frenk, C.S., and White, S.D.M., 1997, *ApJ*, **490**, 493
19. Oort, J.H., 1966, *Bull. Astr. Inst. Netherlands*, **18**, 421
20. Oort, J.H., 1970, *A&A*, **7**, 381
21. Oort, J.H., 1981, *A&A*, **94**, 359
22. Sandage, A., 1986, *ApJ*, **307**, 1
23. Shapiro, P.R., and Field, G.B., 1976, *ApJ*, **205**, 762
24. Verschuur, G.L., 1975, *ARA&A*, **13**, 257
25. Wakker, B.P., and Schwarz, U., 1991, *A&A*, **250**, 484
26. Wakker, B.P., and van Woerden, H., 1991, *A&A*, **250**, 509
27. Wakker, B.P., and van Woerden, H., 1997, it ARA&A, **35**, 217
28. Wolfire, M.G., Hollenbach, D., McKee, C.F., Tielens, A.G.G.M., and Bakes, E.L.O., 1995a, *ApJ*, **443**, 152
29. Wolfire, M.G., McKee, C.F., Hollenbach, D., Tielens, A.G.G.M., 1995b, *ApJ*, **453**, 673
30. Young, L.M., and Lo, K.Y., 1996, *ApJ*, **462**, 203
31. Young, L.M., and Lo, K.Y., 1997a, *ApJ*, **476**, 127
32. Young, L.M., and Lo, K.Y., 1997b, *ApJ*, **490**, 710
33. Zwaan, M.A., Briggs, F.H., Sprayberry, D., and Sorar, E., 1997, *ApJ*, **490**, 173